Endogenous Mas-related G-protein-coupled receptor X1 activates and sensitizes TRPA1 in a human model of peripheral nerves

McMillan, H., Lundy, F. T., Dunne, O. M., Al-Natour, B., Jeanneau, C., About, I., Curtis, T. M., & El Karim, I. (2021). Endogenous Mas-related G-protein-coupled receptor X1 activates and sensitizes TRPA1 in a human model of peripheral nerves. *The FASEB Journal*, *35*(5), Article e21492. https://doi.org/10.1096/fj.202001667RR

Document Version:
Publisher's PDF, also known as Version of record

Queen's University Belfast - Research Portal:
Link to publication record in Queen's University Belfast Research Portal

RESEARCH ARTICLE

Endogenous Mas-related G-protein-coupled receptor X1 activates and sensitizes TRPA1 in a human model of peripheral nerves

Hayley McMillan[1] | Fionnuala T. Lundy[1] [ID] | Orla M. Dunne[1] [ID] | Banan Al-Natour[1,2] |
Charlotte Jeanneau[3] | Imad About[3] | Tim M. Curtis[1] [ID] | Ikhlas El Karim[1] [ID]

[1]School of Medicine, Dentistry and Biomedical Sciences, Queen's University Belfast, UK

[2]Department of Oral Medicine and Oral Surgery, Faculty of Dentistry, Jordan University of Science and Technology, Irbid, Jordan

[3]Aix Marseille Univ, CNRS, ISM, Inst Movement Sci, Marseille, France

Correspondence
Ikhlas El Karim, Wellcome-Wolfson Institute for Experimental Medicine, School of Medicine, Dentistry and Biomedical Sciences, Queen's University Belfast, 97 Lisburn Road, Belfast, BT9 7AE, Northern Ireland, UK.
Email: i.elkarim@qub.ac.uk

Funding information
This study was funded by Animal Free Research UK.

Abstract

Mas-related G-protein-coupled receptor X1 (MrgprX1) is a human-specific Mrgpr and its expression is restricted to primary sensory neurons. However, its role in nociception and pain signaling pathways is largely unknown. This study aims to investigate a role for MrgprX1 in nociception via interaction with the pain receptor, Transient Receptor Potential Ankyrin 1 (TRPA1), using in-vitro and in-vivo human neuronal models. MrgprX1 protein expression in human trigeminal nociceptors was investigated by the immunolabeling of the dental pulp and cultured peripheral neuronal equivalent (PNE) cells. MrgprX1 receptor signaling was monitored by Fura-2-based Ca^{2+} imaging using PNEs and membrane potential responses were measured using FluoVolt™. Immunofluorescent staining revealed MrgprX1 expression in-vivo in dental afferents, which was more intense in inflamed compared to healthy dental pulps. Endogenous MrgprX1 protein expression was confirmed in the in-vitro human PNE model. MrgprX1 receptor signaling and the mechanisms through which it couples to TRPA1 were studied by Ca^{2+} imaging. Results showed that MrgprX1 activates TRPA1 and induces membrane depolarization in a TRPA1 dependent manner. In addition, MrgprX1 sensitizes TRPA1 to agonist stimulation via Protein Kinase C (PKC). The activation and sensitization of TRPA1 by MrgprX1 in a model of human nerves suggests an important role for this receptor in the modulation of nociception.

KEYWORDS

dental pulp, human, MrgprX1, nociception, peripheral neurons

1 | INTRODUCTION

Mas-related G-protein-coupled receptors (Mrgprs) are a complex family of G-protein-coupled receptors (GPCRs), whose physiological function is only partially known. Many of these receptors are selectively expressed in sensory neurons of the dorsal root ganglion (DRG) and trigeminal ganglion (TG)[1-4] and because of this have been suggested to play an important role in nociception and itch.[5-13]

Based on sequence homology, nine subfamilies of mammalian Mrgprs (A-H and X) have been described. The MrgprA, B, and C subfamilies have, up to now, only been

identified in rodents.[2] While MrgprD, E, F, G, and H have been described in rodents, they have clear single gene human orthologs. Using the rodent MrgprA1 sequence as a probe, searches of human genomic libraries later revealed seven primate-specific genes termed MrgprX1-7.[1,3,14] The expression of one of these, MrgprX1, appeared exclusive to humans and similar in sequence to the mouse MrgprA subfamily. However, there is no clear orthologous relationship between individual murine receptors and MrgprX1, which has hampered efforts to understand it.

Ligand activity studies attempted to overcome this issue by identifying rodent receptors with functional homology to MrgprX1, rather than those with a similar sequence. For example, MrgprA3 and MrgprC11 are considered rodent orthologs of MrprX1 simply because they share the same ligands, chloroquine (CQ) and bovine adrenal medulla (8-22) (BAM8-22), respectively.[15] Despite sharing common agonists, murine MrgprA3 and rodent MrgprC11 display distinct pharmacological profiles to human MrgprX1, made evident by the fact that other agonists of human MrgprX1 only weakly activate or have no agonistic activity at rodent MrgprC11 and vice versa.[1,16-19] The same has been shown for mouse MrgprA3 with CQ, with a reported affinity 1000-fold less and an efficacy 2.5-fold less than that of BAM (8-22).[9] However, most interestingly, intrathecal injection of BAM (8-22) decreased inflammatory and neuropathic pain-related behaviors in wild-type mice,[6,20] but were enhanced[20] and prolonged[21] in Mrgpr cluster$^{-/-}$ (Mrgpr$^{-/-}$) mice. Topical application of BAM (8-22) onto the volar forearm of healthy human volunteers produced itch as well as spontaneous nociceptive responses and hypersensitivity to mechanical and thermal stimuli.[10] Given the fact that these data suggest that both MrgprC11 and MrgprA3 act as an analgesic in mice, and MrgprX1 an algetic in humans, extrapolating results from experiments with rodents may not accurately predict the functions of human MrgprX1 receptors.

With no suitable in-vivo model, the bulk of studies on MrgprX1 have utilised overexpression systems and even at such a simplistic level has been shown to differentially modulate neuronal activity. Overexpression of MrgprX1 in rat DRG, hippocampal, and superior cervical ganglion neurons resulted in the inhibition of voltage-gated Ca^{2+} channels, leading to decreased synaptic transmission.[13] Interestingly, inhibition of M-type K^+ channels was also reported in the same cells, which would typically lead to tonic firing.[13] In line with this latter observation, this receptor also induced action potentials after heterologous expression in murine DRG neurons[9] and its activation was found to sensitize transient receptor potential vanilloid 1 (TRPV1) channels in F11 cells stably expressing MrgprX1/TRPV1.[11] Moreover, BAM (8-22) has been reported to mediate the inhibition of heat hypersensitivity and spontaneous pain after nerve injury in a humanized MrgprX1 mouse model.[12] The role, therefore, of MrgprX1 in nociception is not clearly understood. The discrepancies in

the reported functions of MrgprX1 in nociception are likely attributable to the lack of endogenous model systems. As previously mentioned, the majority of studies on MrgprX1 function have been performed following receptor overexpression in different cell types, which may have altered its receptor signaling profile.[22,23]

To better understand its role in nociception, it is crucial to utilize models endogenously expressing MrpgrX1, including in-vivo human neuronal tissue and in-vitro sensory neurons. During the preparation of this manuscript, we identified a recent study that investigated $[Ca^{2+}]_i$ responses in human DRG neurons. They reported that $[Ca^{2+}]_i$ responses were significantly increased following the application of CQ and increased with BAM (8-22), although not significantly in neurons preincubated with a "cocktail" of inflammatory mediators when compared with untreated control neurons.[24] To our knowledge, this is the only study to use human neurons that express MrgprX1 endogenously. Because $[Ca^{2+}]_i$ responses were significantly greater with CQ, which is known to mediate itch in humans,[25] the authors of this study concluded that MrgprX1 is an important player in itch signaling. Using, a human model of peripheral nerves (PNEs) established within our laboratory,[26] the present study aims to look at MrgprX1, with a particular focus on its role in nociception. This is best investigated by studying its coupling with ion channels central to pain and nociception such as TRPA1. TRPA1 is a polymodal channel, expressed in sensory neurons and plays a central role in nociception and inflammatory pain.[27] The role of TRPA1 in mechanical and thermal hyperalgesia has been well documented in a variety of inflammatory pain models.[28-31] In this context, the channel is sensitized by inflammatory mediators via their respective GPCRs, leading to neuronal excitability and development of hyperalgesia and allodynia, characteristics of inflammatory pain.[32] Functional coupling between the mouse ortholog, MrgprC11, and TRPA1 have been reported in heterologous expression systems[33]; however, cross-talk between human MrgprX1 and TRPA1 has yet to be elucidated. As a GPCR that is restricted to sensory neurons, we hypothesized that MrgprX1 modulates neuronal TRPA1 activity to orchestrate nociception and pain signaling.

The aim of this work was to study the in-vivo expression of MrgprX1 in the human dental pulp and to investigate its effect on the activation and sensitization of TRPA1 in an in-vitro human neuronal model.

2 | MATERIALS AND METHODS

2.1 | Immunohistochemical localization of MrgprX1 in human dental pulp

To examine the in-vivo protein expression of MrgprX1, we utilized inflamed human dental pulp as a validated model of human trigeminal nociceptors.[34] Sound and carious teeth with

pulpal inflammation were fixed and processed for routine IHC as previously described.[35] Prior to staining, tooth sections were rehydrated with decreasing ethanol concentrations and antigen retrieval was performed at 98ºC for 30 minutes in 1 mmol/L Tris/0.1 mmol/L EDTA/0.5% Tween. Non-specific binding sites were blocked with phosphate-buffered saline (PBS) containing 1% Bovine Serum Albumin (BSA) for 30 minutes at room temperature. Tooth sections were incubated overnight at 4ºC with rabbit polyclonal antibody against MrgprX1 (1:100; LS-A2756; LS Bio) with or without blocking peptide (LS-E28620; LS Bio). Teeth were co-stained with a monoclonal mouse antibody targeting PGP9.5 (1:250; CL31A3; CEDARLANE) to positively identify nerves innervating the dental pulp. After washing, tissues were incubated for 45 minutes at room temperature with goat anti-rabbit IgG labeled with Alexa-594 and goat anti-mouse IgG labeled Alexa-488 (both 1:200; Life Technologies, Paisley, UK). Some sections were hematoxylin-eosin (H&E) stained and images were captured with an Observer A1 light microscope (Carl Zeiss Microscopy). Fiji v1.53g; an open-source platform for biological image analysis (National Institutes of Health) was used to calculate the integrated density (IntDen) by measuring the total sum of the pixel values in areas of red fluorescence only (MRGXI immunostaining), which fell within the selected threshold range. Threshold ranges were kept consistent per channel across healthy and carious samples. For the quantification, the IntDen was divided by the area of DAPI positive cells on the micrographs. Representative images from three different patient samples were used in the analysis.

2.2 | Generation of peripheral neuronal equivalents (PNEs) from dental pulp stem cells

Human dental pulp stem cells (hDPSCs) obtained from immature third molar teeth were enriched using a fibronectin adherent method and were subsequently differentiated into PNEs as previously described.[26] Briefly, cells were removed from fibronectin-coated plates using trypsin and seeded onto plastic/glassware coated with poly-l-ornithine (0.01%) and laminin (5 μg/mL) and incubated with neurobasal A medium supplemented with B27, GlutaMAX, human basic fibroblast growth factor (40 ng/mL) and epithelial growth factor (20 ng/mL) for 10 days to generate PNEs.

2.3 | Immunocytofluorescence

PNEs were fixed in 4% paraformaldehyde (PFA) for 20 minutes at room temperature and residual PFA was quenched with 0.1 mol/L glycine in PBS. Non-specific binding sites were blocked with 10% normal goat serum supplemented with 0.01% Triton 100-X (PBS-TX) for 1 hour at room temperature, followed by incubation with primary antibody overnight at 4˚C. Afterward, cells were incubated for 1 hour at room temperature with an appropriate secondary antibody. The primary and secondary antibodies used in this study are listed in Table 1. PNEs were mounted using Prolong Gold with DAPI (4',6 diamidino-2-phenylindole) (Invitrogen, UK) to counterstain the nuclei. Images were captured using a Leica SP8 confocal laser scanning microscope (Leica Microsystems). Negative controls were included in each staining whereby the staining procedure was performed in parallel with the other samples but with the omission of the primary antibody. An additional control was carried out for MrgprX1 staining, in which the anti-MrgprX1 antibody was pre-incubated with MRGPRX1 antibody blocking peptide (LS-E28620; LS Bio, Seattle, WA, USA), in excess, for 30 minutes prior to staining as described above.

2.4 | Intracellular Ca^{2+} measurements

A FLIPR Fura-2AM assay was used to study MrgprX1 receptor signaling as well as the involvement of TRPA1 channels in BAM (8-22)-induced Ca^{2+} responses in PNEs. PNEs were grown in 96-well plates, media was removed, and the cells were loaded for 1 hour at 37ºC with 2 μmol/L Fura-2AM in Hanks' solution. For experiments using pharmacological inhibitors, PNEs were pre-treated with inhibitors for 30 minutes before starting the experiment. Intracellular Ca^{2+} was measured using a Flexstation-3 microplate reader (Molecular Devices) with an excitation wavelength of 340 and 380 nm and an emission wavelength of 510 nm. Drugs were added 20 seconds after the start of the experiment using the Flexstation's automated drug delivery system and the recording continued for a further 580 seconds. Changes in intracellular Ca^{2+} were expressed as 340/380 ratios over time. Fura-2 ratiometric data were analyzed by measuring area under the curve (AUC), peak responses (peak minus baseline), and plateau responses (plateau minus baseline) using Prism V8.4.2 (GraphPad Software).

2.5 | Measurement of membrane potential

Membrane depolarization in PNEs grown in 35 mm glass bottom dishes was measured with confocal microfluorimetry. PNEs were loaded with FluoVolt dye 1000X and 100X PowerLoad concentrate (Thermo Fisher Scientific), at concentrations indicated by the manufacturer, in Hanks for 20 minutes at room temperature. PNEs were washed with Hanks and mounted on the stage of an SP5 inverted microscope (Leica microsystems). XY images over time were acquired using an X20 objective (HC PL FLUOTAR 20.0x0.50 DRY) at a frame rate of 1 frame per second using LAS AF software. PNEs were maintained at 37°C by constant

Marker	Species	Catalog No.	Dilution	Company
Primary antibodies				
MAP-2	Rabbit	AB5622	1:500	Millipore, Billerica, MA
TRPV1	Mouse	H00007442-M01	1:100	Abnova, Taipei, TW
PGP9.5	Mouse	CL31A3	1:250	Cedarlane, Burlington, CAN
βIII-Tubulin	Rabbit	04-1049	1:500	Millipore, Billerica, MA
FSP	Mouse	ab 11333	1:500	Abcam, Cambridge, UK
MRGX1	Rabbit	LS-A2756	1:100	LS Bioscience, Seattle, WA
TRPA1	Rabbit	ab 31486	1:100	LS Bioscience Seattle, WA
Nestin	Mouse	LS-B2777	1:250	LS Bioscience Seattle, WA
Secondary antibodies				
Goat anti-rabbit Alexa Fluor 488	Goat	A11008	1:500	Invitrogen, Carlsbad, CA
Goat anti-mouse Alexa Fluor 488	Goat	A11001	1:500	Invitrogen, Carlsbad, CA
Goat anti-rabbit Alexa Fluor 594	Goat	A11012	1:500	Invitrogen, Carlsbad, CA
Goat anti-mouse Alexa Fluor 594	Goat	A11005	1:500	Invitrogen, Carlsbad, CA

perfusion with warmed Hanks. 100 µmol/L BAM (8-22) was added to PNEs after a baseline recording for 90 seconds. For TRPA1 antagonist experiments, PNEs were pre-incubated with 50 µmol/L HC-030031 for 30 minutes prior to the addition of 100 µmol/L BAM (8-22) and 50 µmol/L HC-030031. For positive control experiments, 100 mmol/L potassium chloride (KCl) solution was added.

Membrane fluorescence was expressed as F/F0 ratios, where F represents fluorescence intensity and F0 is the baseline fluorescence prior to the addition of BAM (8-22) or KCl. Pseudo-colored images were acquired on Fiji (v1.53g) where XY stacks were converted to 32-bit format, smoothed, overlaid with a pseudo-colored LUT and the brightness/contrast adjusted.

2.6 | Drugs and Solutions

Hanks' solution contained 140 mmol/L NaCl, 5 mmol/L KCl, 2 mmol/L CaCl$_2$, 1 mmol/L MgCl$_2$, 5 mmol/L D-glucose, 10 mmol/LHEPES (pH 7.4 with NaOH). Reagents in this study were purchased from the following sources: Cinnamaldehyde (CA) (Sigma Aldrich); YM-254890 (Focus Biomolecules); HC-030031 and cyclopiazonic acid (CPA) (Tocris); BAM (8-22), Go 6983 (Hello Bio), Fura2AM (Alfa Aesar). Potassium chloride (Normal HBSS supplemented with 100 Mm KCl (cat no P9541, LOT no 63H031815 Sigma-Aldrich) and FluoVolt™ Membrane Potential Kit: F10488, Thermo Fisher Scientific Massachusetts, USA. All drugs with the exception of BAM (8-22), which was dissolved in Hanks' solution, were dissolved in dimethyl sulfoxide (DMSO) as concentrated stock solutions and diluted at least 200-fold. This produced a final DMSO concentration of 0.5% or less. To test whether DMSO used for dissolving drugs used in calcium imaging is cytotoxic to PNEs, Lactate dehydrogenase (LDH) assay was performed. Cells were treated with 0.5% DMSO for 30 minutes and LDH was measured in the cell supernatant using LDH Cytotoxicity Detection Kit (Sigma Aldrich). The LDH solution (50 µL per well) was then added to 50 µL of cell supernatants in a 96 well plate, in triplicate. The plate was incubated for 30 minutes at room temperature and read at 405 nm using Tecan GENios spectrophotometer and Magellan software. % cytotoxicity was calculated as absorbance of treatment-absorbance of blank divided by the absorbance of dead – absorbance of blank.

2.7 | Statistics analysis

Summary data are presented as mean ± SEM. Statistical comparisons were performed using Prism V8.4.2 (GraphPad Software). Data normality was tested using D'Agostino-Pearson normality omnibus test. Data were analyzed using either Student's t test or by one-way ANOVA with Dunnet's or Bonferroni's post hoc test. In all experiments, $P \leq .05$ was considered statistically significant.

3 | RESULTS

3.1 | MrgprX1 expression in human dental pulp

MrgprX1 expression in healthy and inflamed teeth was investigated with fluorescent IHC as shown in Figure 1. H&E staining was performed on sound and teeth with deep caries to show different stages of inflammation. Dental pulps of sound teeth showed characteristics consistent with the appearance of a healthy pulp, such as an intact odontoblast layer and absence of inflammatory cells (Figure 1A). In teeth with deep caries, features of pulpal inflammation were visible such as inflammatory cell infiltrate and disruption of the odontoblast layer (Figure 1B). Immunofluorescence revealed the expression of PGP9.5 and MrgprX1 in healthy and inflamed teeth. In carious teeth, the expression of MrgprX1 was seen in the odontoblast layer and pulp proper and co-localized with PGP9.5 in nerve bundles (Figure 1H). MrgprX1 expression in the inflamed dental pulp was more intense in comparison to healthy found in sound teeth.

3.2 | Molecular and functional expression of MrgprX1 and TRPA1 in a human model of PNEs

The morphological, molecular, and functional changes that hDPSCs undergo to become PNEs have been recently established within our laboratory.[26] Consistent with the findings
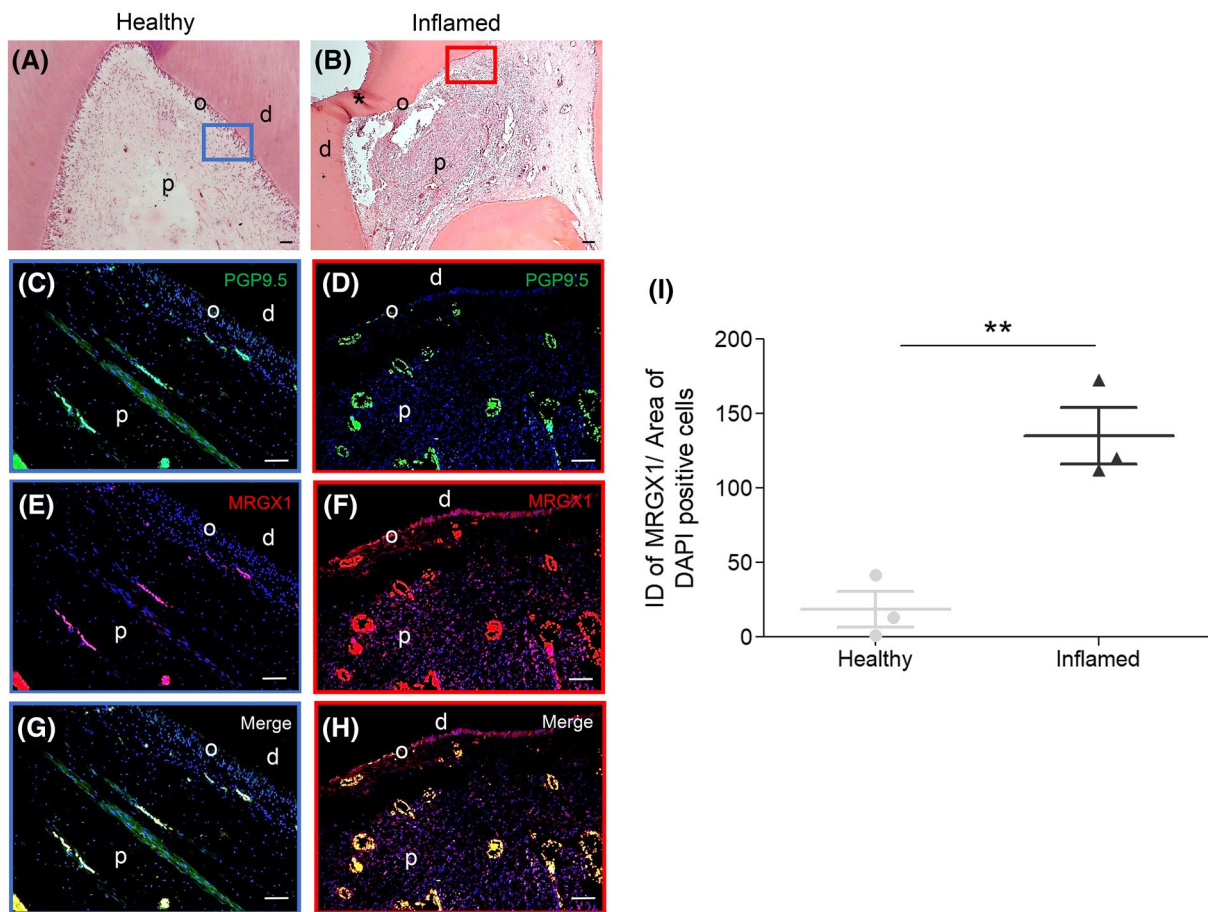

FIGURE 1 Detection of MrgprX1 in healthy and inflamed dental pulp. A and B, hematoxylin-eosin staining of the healthy dental pulp in sound teeth and inflamed pulp in carious teeth. C and E, magnified inset of blue boxed area showing the immunostaining of PGP9.5 (green fluorescence) and MrgprX1 (red fluorescence) in the healthy pulp of sound teeth. D and F, magnified inset of red boxed area showing expression of PGP9.5 and MrgprX1 in the inflamed dental pulp of carious teeth. G and H, PGP9.5 and MrgprX1 co-localized in both healthy and inflamed pulp. I, The integrated density (IntDen) for MrgprX1 divided by the area of DAPI positive cells was significantly increased in the inflamed pulp of carious teeth. **$P \leq .01$, unpaired t-test. N = 3. Scale bars: 100 μm, d (dentin), o (odontoblast), p (dental pulp)
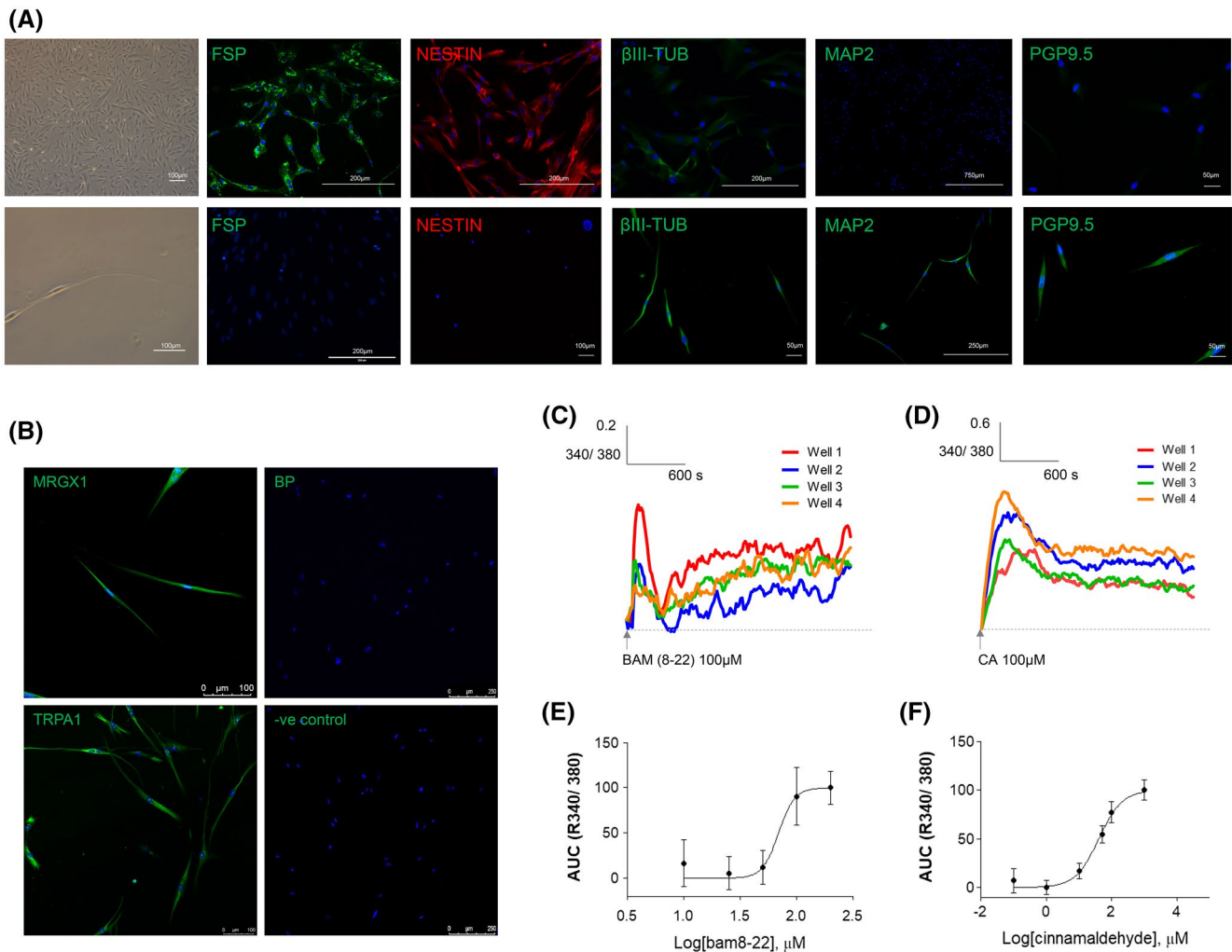
FIGURE 2 Human dental pulp stem cells (hDPSCs) cultured in neurogenic media undergo both morphological and phenotypic changes to become functional peripheral neuronal equivalents (PNEs). A, hDPSCs acquire a fibroblast-like (spindle-shaped) morphology. After 10 days of culture in neurogenic media, hDPSCs lose this shape and adopt a typical bipolar neuronal morphology consisting of a central swollen cell body with long axonal projections. hDPSCs express fibroblast marker, FSP and immature neuronal marker, nestin. Both FSP and nestin expression is lost during neuronal maturation and is no longer expressed in PNEs. Prior to neuronal maturation, hDPSCs do not express mature neuronal markers βIII-tubulin, MAP2 and PGP9.5, which are present in PNE cultures. B, Immunofluorescence confirmed the presence of both MrgprX1 receptors and TRPA1 channels in PNEs co-stained with nuclear stain DAPI. MrgprX1 blocking peptide (BP) and -ve control (secondary antibody only) showed no immunofluorescence. Scale bars: 100 and 250 μm. C and D, Representative 340/380 trace showing PNEs stimulated with MrgprX1 agonist BAM (8-22) (100 μmol/L) and TRPA1 agonist cinnamaldehyde (CA) (100 μmol/L) across four independent wells. E and F, BAM (8-22) and (CA) dose-response curves

described by *Clarke et al*, we show that PNEs adopt a bipolar morphology compatible with that of sensory nerves. Immunocytochemistry was used to assess the protein expression pattern of immature (nestin) and mature (βIII-tubulin, PGP9.5, and MAP2) neuronal-related markers between hDPSCs and PNEs. The data.

confirmed a phenotypic switch from hDPSCs to PNEs during neuronal maturation, evident by the loss of immature neuronal marker, nestin, and gain of mature neuronal markers, βIII-tubulin, MAP2, and PGP9.5. The fibroblast marker, FSP was also included in the characterization panel as fibroblasts are predominant within DPC cultures. The lack of FSP

expression in PNE cultures confirms that the neuronal differentiation process was successful.

Confocal microscopy revealed both MrgprX1 and TRPA1 protein expression in PNEs (Figure 2B). The functional expression of MrgprX1 receptors and TRPA1 channels in PNEs was confirmed by FLIPR Ca^{2+} assays. Representative 340/380 ratio recordings showed that the application of the MRGPRX1 agonist, BAM (8-22), induced an almost instantaneous increase in $[Ca^{2+}]_i$ (Figure 2C). The magnitude of this increase varied from well to well. The levels of $[Ca^{2+}]_i$ began to fall after peaking, but this was followed by a second increase, which was more sustained and in some wells,

reached or succeeded the magnitude of the initial Ca^{2+} transient. Application of the TRPA1 agonist, cinnamaldehyde, also produced a robust increase in $[Ca^{2+}]_i$ which, after peaking, slowly decayed and then came to a plateau above the original baseline, which was approximately 50% of the peak response (Figure 2D). BAM (8-22) and cinnamaldehyde (CA), produced concentration-dependent increases in $[Ca^{2+}]_i$ with EC_{50} values of 69 and 40.6 µmol/L, respectively (Figure 2E,F).

3.3 | MrgprX1 couples to $G\alpha_{q/11}$ proteins in a human model of PNEs

As MrgprX1 receptors were found to be functional in our model of human sensory nerves, we sought to determine the G-protein signaling pathway utilized by MrgprX1. Previous work using MrgprX1 overexpressing cells has shown the involvement of the $G\alpha_{q/11}$ pathway, which is excitatory, or $G\alpha_{i/o}$ signaling which typically inhibits neuronal excitability.[1,13,36-38] We tested the hypothesis that MrgprX1 is excitatory and

confirmed that this receptor couples to the $G\alpha_{q/11}$ pathway in PNEs. As shown in Figure 3A, representative 340/380 ratio recordings and AUC data (Figure 3B) demonstrated that pre-treatment with the $G\alpha_{q/11}$ inhibitor, YM-254890, significantly decreased BAM (8-22) induced increases in $[Ca^{2+}]_i$ when compared to untreated cells. Both the peak and plateau Ca^{2+} responses to BAM (8-22) were significantly reduced by pre-incubating the cells with YM-254890, suggesting that both phases of the response depend upon the activation of the $G\alpha_{q/11}$ signaling pathway (Figure 3C,D). YM-254890 was dissolved to a final DMSO concentration of 0.5% and to test potential cytotoxicity an LDH assay was performed. This showed that 0.5% DMSO is not cytotoxic to PNEs (Figure S1).

3.4 | MrgprX1 signaling activates TRPA1 in PNEs

In addition to being directly activated by a variety of pungent chemicals, TRPA1 is considered a receptor-operated
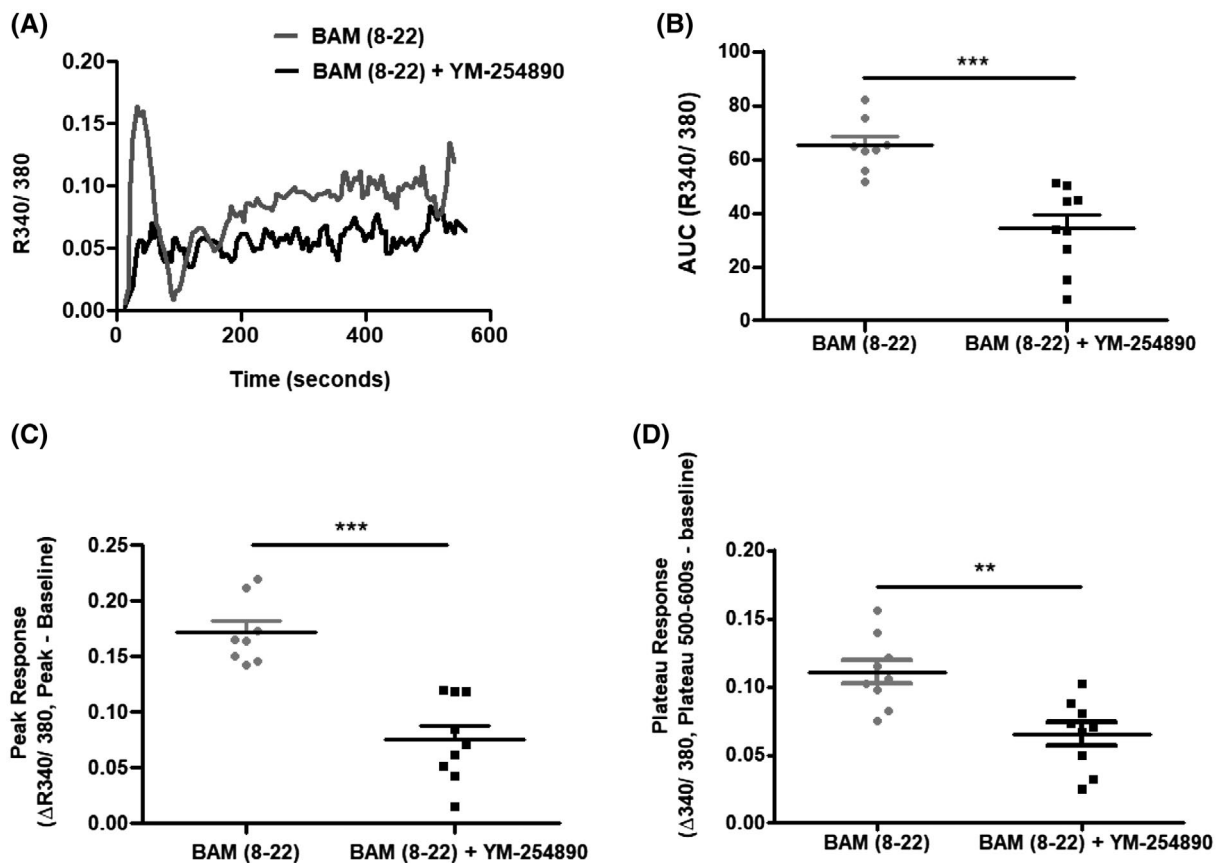

FIGURE 3 MrgprX1 couples to $G\alpha_{q/11}$ proteins in a human model of sensory nerves. A, Representative 340/380 ratio in PNEs stimulated with BAM (8-22) in the presence (black) and absence (grey) of $G\alpha_{q/11}$ inhibitor, YM-254890. B, The initial Ca^{2+} transient that occurred within the first 100 s (measured as peak) of recording in cells stimulated with BAM (8-22) was significantly reduced in cells pre-treated with YM-254890. C and D, AUC of BAM (8-22) induced Ca^{2+} signals over entire recording time (600 s) and mean of last 100 s are also significantly reduced in PNEs pre-treated with YM-254890. **$P \leq .01$, ***$P \leq .001$ represent significant differences between cells pre-treated with and without YM-254890 when challenged with BAM (8-22), unpaired t-test. N = 3

channel that can be modulated indirectly by bradykinin and other GPCR-coupled inflammatory mediators.[31,39] We, therefore, asked whether BAM (8-22) could activate TRPA1 in our human model of sensory neurons. We initially confirmed that 50 μmol/L was an optimal concentration for the inhibition of TRPA1 using the TRPA1 specific antagonist, HC-030031 (Figure 4A). We next stimulated PNEs, pretreated with HC-030031, with BAM (8-22). As shown in Figure 4C,E, TRPA1 inhibition had no effect on the initial Ca^{2+} transient, but significantly reduced the plateau phase of the $[Ca^{2+}]_i$ response. Summary AUC data for the entire recording time (Figure 4B) and measurement of the last 100 seconds of the plateau response (Figure 4E) confirmed these findings. The data suggest that the BAM (8-22) response is in part due to TRPA1 channel activation and that these channels are primarily involved in the plateau phase of the $[Ca^{2+}]_i$ response. To rule out the possibility that TRPA1 is acting as a store-operated Ca^{2+} channel in PNEs, experiments were undertaken using the SERCA pump inhibitor, CPA. PNEs were pre-incubated with HC-030031 and stimulated with CPA to deplete ER Ca^{2+} stores and to activate store-operated Ca^{2+} entry. In response to CPA, PNEs both treated and untreated with HC-030031 displayed an instantaneous increase in $[Ca^{2+}]_i$. This comprised of an initial transient phase and then a more sustained response that remained elevated above the baseline (Figure 4F). While the initial transient phase was similar in both groups, the sustained plateau phase was elevated in PNEs exposed to HC-030031 (Figure 4G-I). These results indicate that TRPA1 does not act as a store-operated Ca^{2+} channel in PNEs, but rather serves to attenuate store-operated Ca^{2+} entry in these cells.

3.5 | MrgprX1 induces membrane depolarization is TRPA1 dependent

To further confirm a role for MrgpX1 in nociception, we tested the ability of BAM (8-22) to modulate the membrane potential of PNEs. This was achieved using the fast voltage-responding fluorescent molecule, FluoVolt[TM]. In positive control experiments, 100 mmol/L potassium chloride (Figure 5A) induced a rapid increase in F/F0, indicating membrane depolarization. This effect was sustained in the continued presence of the high K^+ solution. BAM (8-22) was also found to induce membrane depolarization (Figure 5B), although the response was transient, with F/F0 steadily declining back to baseline levels over the 10-min recording period. This membrane depolarization was completely inhibited in the presence of TRPA1 antagonist, HC-030031 (Figure 5C), suggesting that TRPA1 activation underlies the initiation of this response.

3.6 | MrgprX1 sensitizes TRPA1 responses via the PKC pathway

To further decipher the role of MrgprX1 in neuronal excitability and nociception, we investigated the possibility that TRPA1 is sensitized in the presence of BAM (8-22). As shown in Figure 6A, sustained CA-mediated Ca^{2+} responses were notably larger in PNEs pre-incubated with BAM (8-22). This observation was reflected in measurements of both the AUC (Figure 6B) and the plateau phase of the response (Figure 6C), indicating TRPA1 sensitization subsequent to MrgprX1 activation. This enhanced CA-induced Ca^{2+} response in the presence of BAM (8-22) was substantially reduced in the presence of TRPA1 antagonist, HC-030031 (Figure 6D). To identify the mechanism responsible for TRPA1 sensitization, PNEs were pre-treated with a PKC inhibitor, Go 6983. Figure 6E shows that PKC inhibition blocked the BAM (8-22)-induced sensitization of CA-mediated Ca^{2+} responses in PNEs. AUC (Figure 6F) and mean (Figure 6G) measurements of the plateau response confirmed these findings, indicating that TRPA1 sensitization was PKC dependent.

4 | DISCUSSION

The results of this study demonstrated the endogenous expression and function of MrgprX1 in human sensory neurons. We showed that in a human model of PNEs, MrgprX1 is likely to mediate neuronal excitability and nociception, concurring with previous observations in human volunteers and functional studies in human DRG.[10,24] The primate neuronal-specific expression of MrgprX1 and lack of animal models has limited research on the role of this receptor in nociception and pain but could provide a unique pain relief target in humans that is neuronal specific.

Here we utilized human dental pulp tissue to provide a neuronal model system[26,34] that we found endogenously expresses the sensory-neuron specific receptor, MrgprX1, and characterized its expression for the first time in inflamed and healthy human tissues. The dental pulp is a densely innervated human tissue that mediates pain sensation and is considered a model of human trigeminal nociceptors.[34] The pain from inflamed dental pulp is the worst pain experienced by mankind and is the main reason for patients to seek dental treatment.[40] Our results showed that MrgprX1 expression in pulpal afferents is increased as a result of caries-induced pulpal inflammation, suggesting a role for this receptor in inflammatory pain.

To further study the cellular function and signaling of MrgprX1, we utilized a previously characterized human neuronal model developed in our laboratory derived from
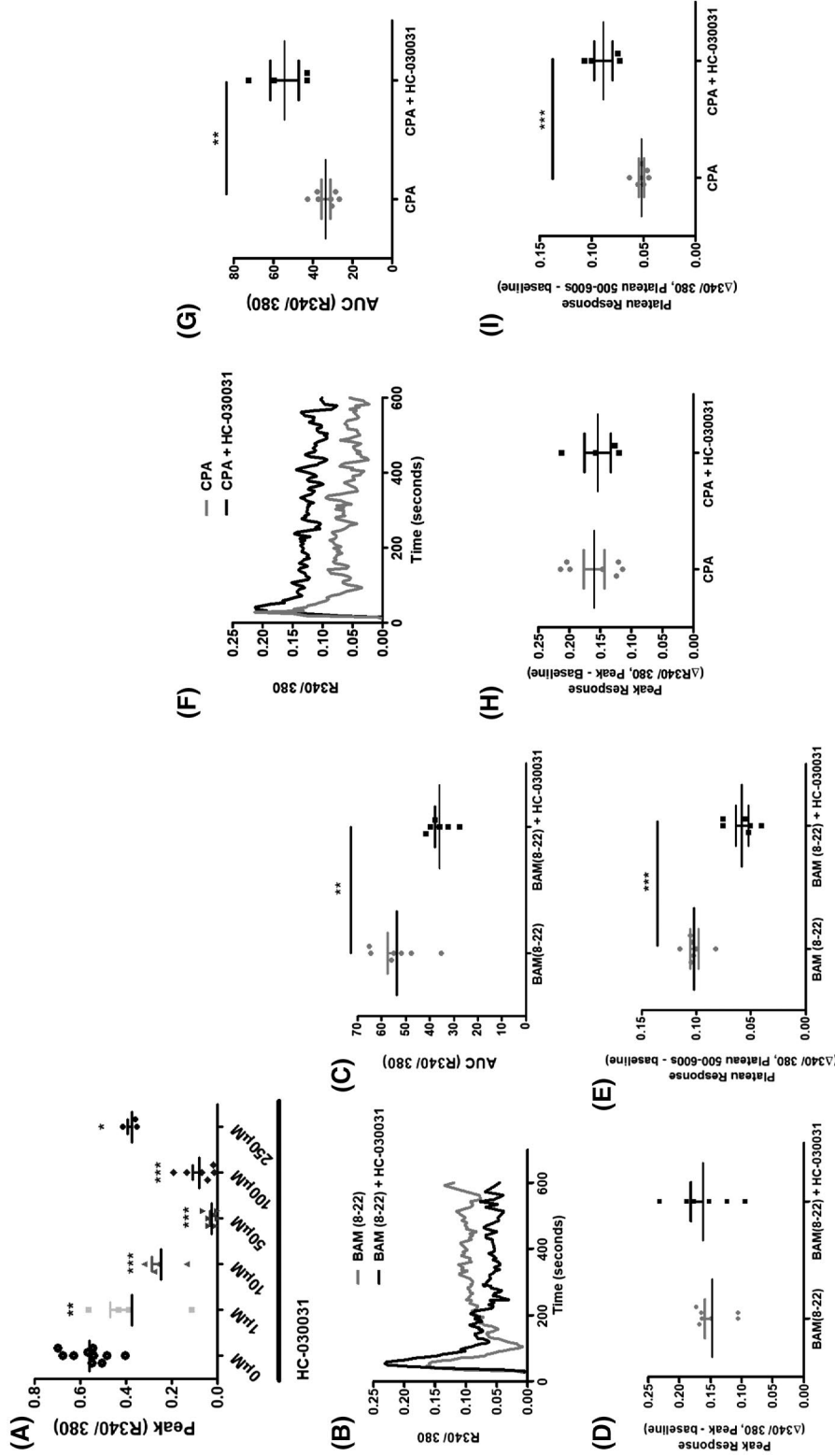
FIGURE 4 MrgprX1 activation modulates TRPA1 channel activity in a human model of sensory nerves. A, Preliminary experiment with PNEs pre-treated with increasing concentrations of TRPA1 antagonist HC-030031 and stimulated with CA, prove 50 μmol/L to be the optimum concentration for blocking TRPA1 channels. Groups were compared using one-way ANOVA, with Dunnett's test, *$P ≤ .05$, **$P ≤ .01$, ***$P ≤ .001$ ($F_{(5, 28)} = 37.71$), N = 3. B, Representative 340/ 380 ratio in PNEs stimulated with BAM (8-22) in the presence (black) and absence (grey) of HC-030031 (50 μmol/L). C, Pre-treatment with HC-030031 did not alter the initial Ca^{2+} transient that occurs within the first 100 s of recording (measured as peak) following the application of BAM (8-22), D and E, AUC of BAM (8-22) mediated Ca^{2+} signals over 600 s of recording and mean of the last 100 s are also significantly reduced in PNEs pre-treated with HC-030031. F, Representative 340/ 380 ratio in PNEs stimulated with CPA with and without HC-03003. G, H and I, AUC, peak and plateau of CPA responses. **$P ≤ .01$, ***$P ≤ .001$ represent significant differences between cells pre-treated with and without HC-030031 when challenged with BAM (8-22), or CPA, unpaired t-test. N = 3
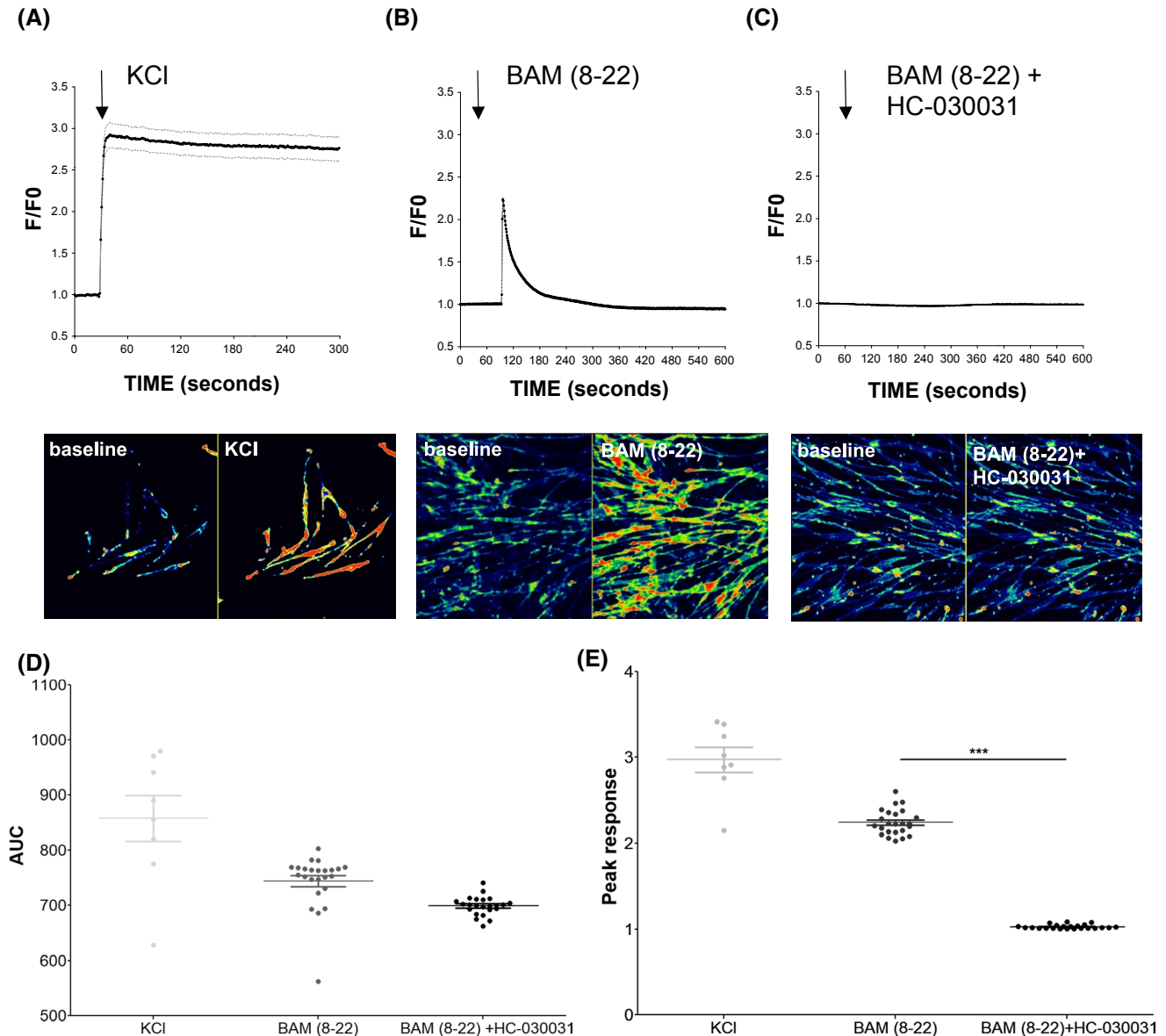
(A) **(B)** **(C)**

FIGURE 5 Effects of BAM on the membrane potential of PNEs using FluoVolt[TM] A, Addition of KCl (100 mmol/L) increased F/F0 in 8 PNEs analyzed. Corresponding pseudo-colored panels show a change in fluorescence intensity with KCl application in PNEs. B, MrgprX1 agonist BAM (8-22) (100 μmol/L) increased F/F0 in 24 PNEs analyzed. Corresponding pseudo-colored panels show changes in fluorescence intensity with BAM (8-22) application in PNE. C, BAM (8-22) responses were inhibited in the presence of the TRPA1 antagonist HC-030031 (50 μmol/L) in 23 PNEs analyzed. Corresponding pseudo-colored panels show no obvious change in fluorescence intensity with BAM (8-22) + HC-030031 application in PNEs. Time of addition of all compounds was as indicated by black arrows. Mean ± SEM (indicated by dashed lines). D and E, Area under curve (AUC) and Peak response analysis of KCl, BAM (8-22), BAM (8-22) + HC-030031 response. Mean ± SEM, each dot represents a ROI. Peak response is significantly decreased in BAM (8-22) +HC-03001 compared to BAM (8-22) alone, ***$P \leq .0001$, unpaired t-test

dental pulp stem cells.[26] Neuronal differentiation of dental pulp stem cells is well documented in the literature[26,41-46] and their use as a tool to study neuronal signaling has been previously established.[44,46] Using this model, we confirmed the functional expression of MrgprX1 and its coupling to the $G\alpha_{q/11}$ excitatory pathway in agreement with studies in overexpressing cell lines.[1,11] This excitatory and nociceptive role is in line with our data on the expression of this receptor in the inflamed dental pulp of carious teeth and in two human studies that showed increased pain and sensitization

and increased Ca^{2+} responses following the application of BAM (8-22).[10,24]

An important finding from this study was the observed coupling between MrgprX1 and TRPA1. TRPA1 is a poly-modal ion channel that plays an important role in inflammatory nociception.[27,31] TRPA1 expression has previously been reported in the dental pulp and a human neuronal model[26,47] and its expression is known to be modulated by GPCR signaling to mediate inflammatory pain.[30,31,48,49] Throughout this manuscript, we have consistently shown that BAM
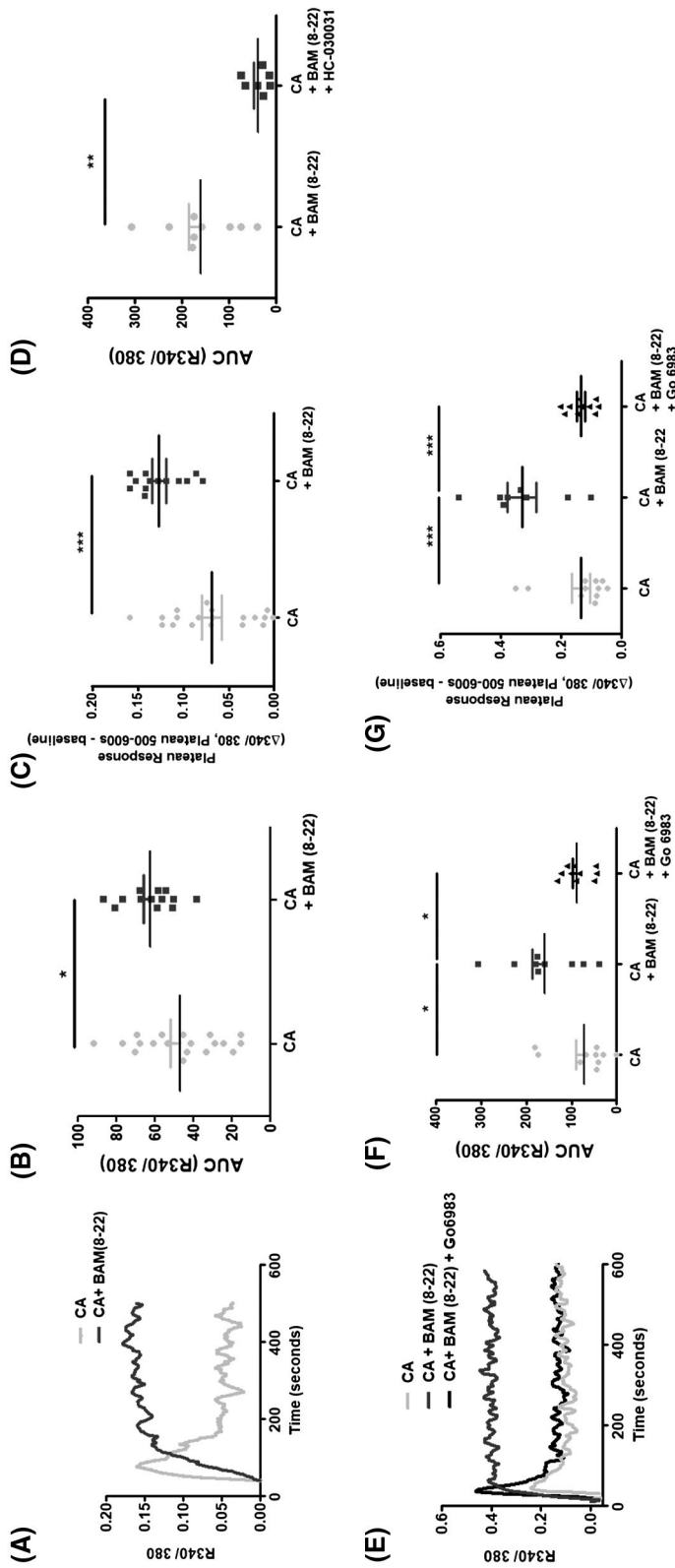
FIGURE 6 Activation of MrgprX1 sensitizes TRPA1 channels in a PKC-dependent manner. A, Representative 340/380 ratio in PNEs stimulated with CA in the presence (dark grey) and absence (grey) of BAM (8-22). B, AUC of the entire recording time (600 s) and (C) mean of the last 100 s demonstrates that pre-treatment with BAM (8-22) significantly increases and prolongs CA-induced Ca^{2+} responses. D, Pre-treatment with HC-030031 significantly reduces BAM (8-22) mediated TRPA1 sensitization. Groups were compared using unpaired t-test, $*P \leq .05$, $**P \leq .01$, $***P \leq .001$. N = 3. E, Representative 340/380 ratio in PNEs stimulated with CA in the presence of extracellular buffer, hanks (grey), BAM (8-22) (dark grey), and BAM (8-22) + PKC inhibitor Go 6983 (black). F and G, AUC of CA induced Ca^{2+} responses over 600 s and mean of last 100 s are significantly increased in the presence of BAM (8-22); however, this increased response is diminished in the presence of Go 6983. $*P \leq .05$, ($F_{(2, 26)} = 11.51$), $***P \leq .001$ ($F_{(2, 26)} = 5.72$), one-way ANOVA, with Bonferroni's test. N = 3

(8-22)-mediated Ca^{2+} responses involve two main phases: an initial transient phase and a plateau phase, the latter being more sustained and often exceeding the transient phase. This response is identical to Putney's first descriptions of receptor-regulated Ca^{2+} entry, where the transient phase was a result of Ca^{2+} released from IP_3-sensitive stores and the plateau phase is due to Ca^{2+} entry from membrane ion channels.[50] In PNEs, pharmacological inhibition of TRPA1 with HC-030031 had no effect on the transient (Ca^{2+} release phase), but significantly reduced the plateau (Ca^{2+} influx) phase of the BAM (8-22) responses. Our findings strongly suggest that BAM (8-22)-induced TRPA1 activation in PNEs occurs through a receptor- rather than a store-operated pathway. Indeed, blockade of TRPA1 channels with HC-030031 enhanced, rather than inhibited, store-operated Ca^{2+} entry evoked by the SERCA pump inhibitor CPA. This is consistent with a study by Albarrán and colleagues who reported that the silencing of TRPA1 channel expression in MEG01 cells enhanced thapsigargin-induced Ca^{2+} entry without altering the release of Ca^{2+} from intracellular stores.[51] Their data showed that TRPA1 normally inhibits store-operated Ca^{2+} influx by reducing the association between STIM1 and Orai channels. Although the exact mechanisms through which MrgprX1 and TRPA1 are functionally coupled in PNEs have yet to be fully elucidated, a number of receptor-regulated pathways may be of relevance. One of the first major events in the agonist activation of $G\alpha_{q/11}$ coupled receptors like MrgprX1 is the activation of PLC and hence the breakdown of PIP_2 into IP_3 and DAG. Earlier findings by Bandell and co-workers showed direct activation of TRPA1 with 1-oleoyl-2-acetyl-sn-glycerol, a cell- permeable analoug of DAG.[30] DAG could also mediate PKC-dependent phosphorylation of TRPA1, causing its activation. However, bone-fide TRPA1 activation by PKC has yet to be observed. In addtion, studies have demonstrated that PIP_2 inhibits TRPA1.[11,48,52] This would suggest that TRPA1 activity is normally suppressed and that PIP_2 degradation by PLC results in the release of TRPA1 from inhibition, causing TRPA1 to open. Regardless of the mechanism by which MrgprX1 activates TRPA1, our FluoVolt data clearly showed that BAM (8-22) can induce excitable effects in PNEs through a TRPA1-dependent mechanism. During our recordings, the membrane potential of PNEs was quiescent under resting conditions, and therefore further optimization of these cultures and/or methodological developments will be needed to investigate the effects of the MrgprX1/TRPA1 signaling axis on repetitive action potential generation in these cells.

Using a validated PKC inhibitor, we show that MrgprX1 sensitizes TRPA1 channels in a PKC-dependent manner. We showed that Ca^{2+} signals in response to the TRPA1 agonist, CA, are greatly enhanced when cells were pre-treated with BAM (8-22) and this response was diminished in the presence of the PKC inhibitor, Go 6983. Activation of PKC

has been implicated in the sensitization of family member TRPV1 by a variety of agents, including BAM (8-22).[11,53,54] In agreement with previous work,[55] our data suggest PKC-dependent sensitization of TRPA1 by MrgprX1, which is in disagreement with findings using other GPCR agonists[39,48] that have shown that PLC-dependent hydrolysis of phosphatidylinositol bisphosphate (PIP_2) is the mechanism responsible for TRPA1 sensitization by PAR-2 and bradykinin receptors.

Sensitization of TRPA1 with BAM (8-22) is not unexpected if MrgprX1 is to play a role in nociception and inflammatory pain. TRPA1 exists as a major target for pain relief but the expression of this ion channel both inside and outside the somatosensory system, in addition to having a wide range of physiological functions,[56,57] may limit its role in pain relief drug discovery. Therefore, modulation of TRPA1 by neuron-specific MrgprX1 may provide a more specific pain target with potentially fewer side-effects.

In conclusion, our data have provided evidence for endogenous MrgprX1 expression and function in human sensory neurons. The study has provided valuable insights into MrgprX1 coupling to TRPA1 that merits further investigation in human clinical nociceptive pain models. As many receptors and channels infamously known for their role in pain are too expressed in itch-specific neurons,[15] we acknowledge that the cross-talk between MrgprX1 and TRPA1 could be part of nociception signaling pathway in itch and pain.

CONFLICT OF INTEREST

The authors have stated explicitly that there are no conflicts of interest in connection with this article.

AUTHOR CONTRIBUTIONS

I. El karim, F. Lundy and T. Curtis designed research; H. McMillan, O. Dunne, B. Al-Natour, I. About and C Jeanneau performed research; H. McMillan, O. Dunne, I El karim, analyzed the data H. McMillan, I. El karim, F. Lundy, T. Curtis wrote the paper.

ORCID

Fionnuala T. Lundy https://orcid.org/0000-0003-3150-1150
Orla M. Dunne https://orcid.org/0000-0003-0769-4247
Tim M. Curtis https://orcid.org/0000-0003-1543-2781
Ikhlas El Karim https://orcid.org/0000-0002-5314-7378

REFERENCES

1. Lembo PMC, Grazzini E, Groblewski T, et al. Proenkephalin A gene products activate a new family of sensory neuron–specific GPCRs. *Nat Neurosci*. 2002;5(3):201-209.
2. Zylka MJ, Dong X, Southwell AL, Anderson DJ. Atypical expansion in mice of the sensory neuron-specific Mrg G protein-coupled receptor family. *Proc Natl Acad Sci USA*. 2003;100(17):10043-10048.

3. Dong X, Han S-K, Zylka MJ, Simon MI, Anderson DJ. A diverse family of GPCRs expressed in specific subsets of nociceptive sensory neurons. *Cell*. 2001;106(5):619-632.

4. Flegel C, Schöbel N, Altmüller J, et al. RNA-Seq Analysis of Human Trigeminal and Dorsal Root Ganglia with a Focus on Chemoreceptors. *PLoS One*. 2015;10(6):e0128951

5. Reddy VB, Azimi E, Chu L, Lerner EA. Mas-Related G-Protein Coupled Receptors and Cowhage-Induced Itch. *J Invest Dermatol*. 2018;138(2):461-464.

6. He SQ, Li Z, Chu YX, et al. MrgC agonism at central terminals of primary sensory neurons inhibits neuropathic pain. *Pain*. 2014;155(3):534-544.

7. Guan Y, Yuan F, Carteret AF, Raja SN. A partial L5 spinal nerve ligation induces a limited prolongation of mechanical allodynia in rats: an efficient model for studying mechanisms of neuropathic pain. *Neurosci Lett*. 2010;471(1):43-47.

8. Han L, Ma C, Liu Q, et al. A subpopulation of nociceptors specifically linked to itch. *Nat Neurosci*. 2013;16(2):174-182.

9. Liu Q, Tang Z, Surdenikova L, et al. Sensory neuron-specific GPCR Mrgprs are itch receptors mediating chloroquine-induced pruritus. *Cell*. 2009;139(7):1353-1365.

10. Sikand P, Dong X, LaMotte RH. BAM8-22 peptide produces itch and nociceptive sensations in humans independent of histamine release. *J Neurosci*. 2011;31(20):7563-7567.

11. Solinski HJ, Zierler S, Gudermann T, Breit A. Human sensory neuron-specific Mas-related G protein-coupled receptors-X1 sensitize and directly activate transient receptor potential cation channel V1 via distinct signaling pathways. *J Biol Chem*. 2012;287(49):40956-40971.

12. Li Z, Tseng P-Y, Tiwari V, et al. Targeting human Mas-related G protein-coupled receptor X1 to inhibit persistent pain. *Proc Natl Acad Sci*. 2017;114(10):E1996-E2005.

13. Chen H, Ikeda SR. Modulation of ion channels and synaptic transmission by a human sensory neuron-specific G-protein-coupled receptor, SNSR4/mrgX1, heterologously expressed in cultured rat neurons. *J Neurosci*. 2004;24(21):5044-5053.

14. Choi SS, Lahn BT. Adaptive evolution of MRG, a neuron-specific gene family implicated in nociception. *Genome Res*. 2003;13(10):2252-2259.

15. Meixiong J, Dong X. Mas-related G protein-coupled receptors and the biology of itch sensation. *Annu Rev Genet*. 2017;51:103-121.

16. Solinski HJ, Gudermann T, Breit A. Pharmacology and signaling of MAS-related G protein-coupled receptors. *Pharmacol Rev*. 2014;66(3):570-597.

17. Schmidt R, Butterworth J, O'Donnell D, Santhakumar V, Tomaszewski M. Cyclic dimers of C-TERMINAL γ2-MSH analogs as selective antagonists of the human sensory nerve-specific receptor (SNSR-4). *Adv Exp Med Biol*. 2009;611:111-112.

18. Bayrakdarian M, Butterworth J, Hu Y-J, Santhakumar V, Tomaszewski MJ. Development of 2,4-diaminopyrimidine derivatives as novel SNSR4 antagonists. *Bioorg Med Chem Lett*. 2011;21(7):2102-2105.

19. Kunapuli P, Lee S, Zheng W, et al. Identification of small molecule antagonists of the human mas-related gene-X1 receptor. *Anal Biochem*. 2006;351(1):50-61.

20. Guan L, Tang R, Anderson D. Mas-related G-protein-coupled Receptors Inhibit Pathological Pain in Mice. *Proc Natl Acad Sci USA*. 2010;107(36):15933-15938.

21. He SQ, Han L, Li Z, et al. Temporal changes in MrgC expression after spinal nerve injury. *Neuroscience*. 2014;261:43-51.

22. Kenakin T. Differences between natural and recombinant G protein-coupled receptor systems with varying receptor/G protein stoichiometry. *Trends Pharmacol Sci*. 1997;18(12):456-464.

23. Kenakin T. Collateral efficacy as a pharmacological problem applied to new drug discovery. *Expert Opin Drug Discov*. 2006;1(7):635-652.

24. Castro J, Harrington AM, Lieu TM, et al. Activation of pruritogenic TGR5, MRGPRA3, and MRGPRC11 on colon-innervating afferents induces visceral hypersensitivity. *JCI Insight*. 2019;4(20):131712.

25. Sowunmi A, Walker O, Salako LA. PRURITUS and antimalarial drugs in Africans. *Lancet*. 1989;334(8656):213.

26. Clarke R, Monaghan K, About I, et al. TRPA1 activation in a human sensory neuronal model: relevance to cough hypersensitivity? *Eur Respir J*. 2017;50(3):1700995.

27. Bautista DM, Pellegrino M, Tsunozaki M. TRPA1: A Gatekeeper for Inflammation. *Annu Rev Physiol*. 2013;75(1):181-200.

28. Petrus M, Peier AM, Bandell M, et al. A Role of TRPA1 in mechanical hyperalgesia is revealed by pharmacological inhibition. *Mol Pain*. 2007;3:3-40.

29. Eid SR, Crown ED, Moore EL, et al. HC-030031, a TRPA1 Selective Antagonist, Attenuates Inflammatory- and Neuropathy-Induced Mechanical Hypersensitivity. *Mol Pain*. 2008;4:4-48.

30. Bandell M, Story GM, Hwang SW, et al. Noxious cold ion channel TRPA1 Is activated by pungent compounds and bradykinin. *Neuron*. 2004;41(6):849-857.

31. Bautista DM, Jordt SE, Nikai T, et al. TRPA1 mediates the inflammatory actions of environmental irritants and proalgesic agents. *Cell*. 2006;124(6):1269-1282.

32. Yekkirala AS. Two to tango: GPCR oligomers and GPCR-TRP channel interactions in nociception. *Life Sci*. 2013;92(8–9):438-445.

33. Wilson SR, Gerhold KA, Bifolck-Fisher A, et al. TRPA1 is required for histamine-independent, mas-related g protein-coupled receptor-mediated itch. *Nat Neurosci*. 2011;14(5):595-602.

34. Fehrenbacher JC, Sun XX, Locke EE, Henry MA, Hargreaves KM. Capsaicin-evoked iCGRP release from human dental pulp: A model system for the study of peripheral neuropeptide secretion in normal healthy tissue. *Pain*. 2009;144(3):253-261.

35. Téclès O, Laurent P, Zygouritsas S, et al. Activation of human dental pulp progenitor/stem cells in response to odontoblast injury. *Arch Oral Biol*. 2005;50(2):103-108.

36. Breit A, Gagnidze K, Devi LA, Lagacé M, Bouvier M. Simultaneous activation of the δ opioid receptor (δOR)/sensory neuron-specific receptor-4 (SNSR-4) hetero-oligomer by the mixed bivalent agonist bovine adrenal medulla peptide 22 activates SNSR-4 but inhibits δOR signaling. *Mol Pharmacol*. 2006;70(2):686-696.

37. Solinski HJ, Boekhoff I, Bouvier M, Gudermann T, Breit A. Sensory neuron-specific mas-related gene-X1 receptors resist agonist-promoted endocytosis. *Mol Pharmacol*. 2010;78(2):249-259.

38. Burstein ES, Ott TR, Feddock M, et al. Characterization of the Mas-related gene family: structural and functional conservation of human and rhesus MrgX receptors. *Br J Pharmacol*. 2006;147(1):73-82.

39. Wang S, Dai Y, Fukuoka T, et al. Phospholipase C and protein kinase A mediate bradykinin sensitization of TRPA1: a molecular mechanism of inflammatory pain. *Brain*. 2008;131(5):1241-1251.

40. Matthews B, Vongsavan N. Interactions between neural and hydrodynamic mechanisms in dentine and pulp. *Arch Oral Biol*. 1994;39(Suppl):87S-95S.

41. Gronthos S, Brahim J, Li W, et al. Stem cell properties of human dental pulp stem cells. *J Dental Res*. 2002;81(8):531-535.

42. Arthur A, Rychkov G, Shi S, Koblar SA, Gronthos S. Adult human dental pulp stem cells differentiate toward functionally active neurons under appropriate environmental cues. *Stem Cells*. 2008;26(7):1787-1795.

43. Bonnamain V, Thinard R, Sergent-Tanguy S, et al. Human dental pulp stem cells cultured in serum-free supplemented medium. *Front Physiol*. 2013;4:357.

44. Gervois P, Struys T, Hilkens P, et al. Neurogenic maturation of human dental pulp stem cells following neurosphere generation induces morphological and electrophysiological characteristics of functional neurons. *Stem Cells Dev*. 2015;24(3):296-311.

45. Young FI, Telezhkin V, Youde SJ, et al. Clonal heterogeneity in the neuronal and glial differentiation of dental pulp stem/progenitor cells. *Stem Cells Int*. 2016;2016:1-10.

46. Li D, Zou X-Y, El-Ayachi I, et al. Human dental pulp stem cells and gingival mesenchymal stem cells display action potential capacity in vitro after neuronogenic differentiation. *Stem Cell Rev Reports*. 2019;15(1):67-81.

47. El Karim IA, McCrudden MTC, McGahon MK, et al. Biodentine reduces tumor necrosis factor alpha–induced TRPA1 expression in odontoblastlike cells. *J Endod*. 2016;42(4):589-595.

48. Dai Y, Wang S, Tominaga M, et al. Sensitization of TRPA1 by PAR2 contributes to the sensation of inflammatory pain. *J Clin Invest*. 2007;117(7):1979-1987.

49. Meents JE, Fischer MJM, McNaughton PA. Sensitization of TRPA1 by protein kinase A. *PLoS One*. 2017;12(1).

50. Putney JW. A model for receptor-regulated calcium entry. *Cell Calcium*. 1986;7(1):1-12.

51. Albarrán L, Lopez JJ, Dionisio N, Smani T, Salido GM, Rosado JA. Transient receptor potential ankyrin-1 (TRPA1) modulates store-operated Ca 2+ entry by regulation of STIM1-Orai1 association. *Biochim Biophys Acta - Mol Cell Res*. 2013;1833(12):3025-3034.

52. Kim D, Cavanaugh EJ, Simkin D. Inhibition of transient receptor potential A1 channel by phosphatidylinositol-4,5-bisphosphate. *Am J Physiol Cell Physiol*. 2008;295(1):C92.

53. Premkumar LS, Ahern GP. Induction of vanilloid receptor channel activity by protein kinase C. *Nature*. 2000;408(6815):985-990.

54. Bhave G, Hu H-J, Glauner KS, et al. Protein kinase C phosphorylation sensitizes but does not activate the capsaicin receptor transient receptor potential vanilloid 1 (TRPV1). *Proc Natl Acad Sci USA*. 2003;100(21):12480-12485.

55. Brackley AD, Gomez R, Guerrero KA, et al. A-kinase anchoring protein 79/150 scaffolds transient receptor potential a 1 phosphorylation and sensitization by metabotropic glutamate receptor activation. *Sci Rep*. 2017;7(1):1842.

56. Kremeyer B, Lopera F, Cox JJ, et al. A gain-of-function mutation in TRPA1 causes familial episodic pain syndrome. *Neuron*. 2010;66(5):671-680.

57. Aubdool AA, Graepel R, Kodji X, et al. TRPA1 is essential for the vascular response to environmental cold exposure. *Nat Commun*. 2014;5(1):5732.

SUPPORTING INFORMATION

Additional Supporting Information may be found online in the Supporting Information section.